WILEY | Hindawi

Research Article

Operation and Testing of Indirect Field Oriented Control of Asymmetrical Six-Phase Open-Ended Winding Induction Machine Using Hardware-in-Loop (HIL) Emulator

Arif Iqbal [ID],[1] **Farhad Ilahi Bakhsh** [ID],[2] **and Girish Kumar Singh** [ID][3]

[1]*Electrical Engineering Department, Rajkiya Engineering College, Ambedkar Nagar, India*
[2]*Electrical Engineering Department, National Institute of Technology, Srinagar, India*
[3]*Electrical Engineering Department, Indian Institute of Technology, Roorkee, India*

Correspondence should be addressed to Arif Iqbal; arif.iqbal.in@gmail.com

This study deals with an asymmetrical six-phase open-ended winding induction machine in closed loop operation using indirect field-oriented control scheme. The closed loop scheme has been developed by using the two axis (d-q) modeling of six-phase induction machine in rotating synchronous reference frame and can be easily extended to any multiphase machine having the stator winding which are the multiple of three. Operation under steady-state is considered to develop the phasor diagram in closed loop operation of machine in the motoring mode. The performance of the asymmetrical six-phase induction machine (opened ended winding) is investigated in the entire four-quadrant operation. The complete machine drive system was developed by using MATLAB/Simulink, which was used to obtain analytical results in different modes. Furthermore, the analytical results in the motoring mode were experimentally validated through real-time simulation by using Typhoon hardware-in-loop (HIL) emulator.

1. Introduction

The utility of induction motor drive can be found in almost every industrial application with a wide power range (upto to 1 MW). But the use of induction motor drive is not suitable for very high power applications (multi-MW range) [1]. This limitation has diverted the attention of researchers and many new findings have been reported in the available literature. The reported development is both from the machine as well as input power supply. From the machine side, it is a common strategy to reconfigure the stator winding to realize a multi-phase (more than three-phase) motor, thereby increasing the power handling capability [2] together with improved reliability and reducing harmonics (both time and space) when compared with its three-phase equivalent. The input power segregation from the connected converter circuit may be substantially improved with the open-ended winding configuration of the multiphase motor (i.e. six-phase in this study) resulting in enhanced reliability of the system.

With the ongoing technological developments [3], a three-phase induction motor with open-ended winding configuration has been extensively investigated from last few years [4]. Operation of the motor drives was presented by using newly developed space-vector pulse width modulation (SVPWM) scheme [5], and a reduced power loss (by 4.5–11%) was reported [6]. The authors in reference [7] have developed two schemes of SVPWM to drive open-ended winding induction motor (OEWIM), and an improved harmonic performance was reported for a wide speed range. Motor conversion efficiency was maintained high over a wider load setting and operating frequencies by using the dual inverter equipped with a floating bridge capacitor [8]. Furthermore, the system was analysed to develop a fault-tolerant OEWIM drive with the possible outage of converter switches [9]. For the improvement of motor performance with higher conversion efficiency for a wide range of load and in high-speed region, OEWIM operation was considered at a constant power factor at fundamental value [10]. A

robust field-oriented control was developed to operate OEWIM, and an improved efficiency was reported around base speed and at high torque [11]. Induction motor drive was also investigated by applying predictive control (PTC) [12], wherein for minimal flux errors, a comparison between flux error objectives and a set of weighting factors (WFs) was carried out. The predefined WFs were used for the final selection of voltage vectors (VVs). OEWIM drive using enhanced PTC [13] was presented, in which flux assignment was eliminated and space vector-based control of stator flux was introduced to achieve the combined control of flux and torque. The authors in [4] have addressed OEWIM drive applicable for electric vehicles, wherein two algorithms of rotor flux were proposed, i.e., the motor loss minimization algorithm (MLM algorithm) and the maximum power sharing capability algorithm (MPSC algorithm). It was concluded that MLM and MPSC algorithms are suitable for optimal efficiency and maximized power sharing of input dual inverter, respectively, in a wide operating range of motor.

The operation of the multiphase motor with open-ended winding is reported through the development of various modulating schemes using the concept of space vector modulation [14, 15] and carrier-based pulse width modulation (PWM) [16] for five-phase and six-phase induction motor [17]. It is noted that the available literature on multiphase open-ended winding induction motor deals with the operation in open loop. In contrast to this, it is usual practice to realize the motor operation in closed loop. In this regard, the technique of indirect field oriented control (i.e., vector control scheme) of induction motor is well adopted in high performance industrial application. The scheme of vector control facilitates an independent control of torque and flux component of motor current similar to a separately excited DC motor, resulting in significant improvement in operating performance. Although the vector control scheme is well developed and investigated in available literature [18, 19], stator windings are connected in dual star. But the development of this scheme for asymmetrical six-phase open-ended winding induction motor has not been reported so far to the best of the authors' knowledge. This research gap has been addressed through the development and investigation of vector control scheme (i.e., indirect field-oriented control) for asymmetrical six-phase open-ended winding induction motor in the following section. The mathematical model of the complete machine drive system was developed by using MATLAB/Simulink, which was used to obtain analytical results in entire four quadrant operation. The analytical results in the motoring mode were experimentally validated though real-time simulation [20] by using Typhoon hardware-in-loop (HIL) emulator.

Section 2 presents the mathematical modeling of six-phase induction machine (i.e., the two axis d-q model) in arbitrary reference frame. Section 3 mathematically develops the proposed control scheme in synchronous reference frame applicable for an asymmetrical six-phase open-ended winding induction machine. Implementation of control scheme is highlighted in Section 4. Machine operation in entire four quadrant operation is presented in Section 5 with

their experimental validation in the motoring mode in Section 6. Presented work has been concluded with some significant remarks in Section 7.

2. Mathematical Modeling

For the purpose to realize a six-phase motor, it is a common strategy to reconfigure the stator winding of existing three-phase machine into the two sets of three-phase, namely, A and X using the concept of phase belt split [2]. The resultant winding sets A and X are used to realize a six-phase winding which are asymmetrically displaced by an angle ξ (=30 degree). Asymmetry in six-phase winding results in the cancellation of lower order harmonics (both space and time), and a smooth motor operation is achieved with reduced torque pulsation [2, 21–23]. Each three-phase end terminals of each winding set A and X (a b c and aa' bb' cc' are the end terminals of winding set A; x y z and xx' yy' zz' are the end terminals of winding set X) are connected to an independent inverter (inverters 1 and 2 connected to winding set A; inverters 3 and 4 are connected to winding set X) to feed the induction machine as shown in Figure 1. It is important to mention here that the phase difference of 180 degree electrical is maintained between voltage vector phasor of both inverters connected to each winding set A and X. The motor pole voltages v_{sa}, v_{sb}, v_{sc} and v_{sx}, v_{sy}, v_{sz} are associated with the winding set A and X, respectively. These pole voltages are independently attributed by the connected inverter at open ends of winding set A and X. Pole voltages and currents together with their equivalent in d-q axes are defined in the Appendix.

Voltage equations of six-phase induction motor are preferably written in arbitrary reference frame as follows:

$$
\begin{aligned}
v_{dqk} &= r_{sk}i_{dqk} + \omega_k\lambda_{dqk} + p\lambda_{dqk}, \\
v_{qr} &= r_{qr}i_{qr} + (\omega_k - \omega_r)\lambda_{dr} + p\lambda_{qr}, \\
v_{dr} &= r_{dr}i_{dr} - (\omega_k - \omega_r)\lambda_{qr} + p\lambda_{dr}, \\
v_{dqk} &= \begin{bmatrix} v_{dk} & v_{qk} \end{bmatrix}^T, \\
\lambda_{dqk} &= \begin{bmatrix} \lambda_{dk} & -\lambda_{qk} \end{bmatrix}^T, \\
r_{dqk} &= \begin{bmatrix} r_{dk} & r_{qk} \end{bmatrix}^T,
\end{aligned}
\tag{1}
$$

for $k = 1, 2$ for winding set A and X, respectively.

It is important to mention here that that in the stator equation, the voltage and current are constituted by two inverters connected at the open-ended winding set A or X and are defined in the Appendix. Equation of flux linkage in terms of motor currents is defined as

$$
\lambda = Li, \tag{2}
$$

where

$$
i = \begin{bmatrix} i_{dqk} & i_{dqk} \end{bmatrix}^T, \tag{3A}
$$

$$
\lambda = \begin{bmatrix} \lambda_{dqk} & \lambda_{dqk} \end{bmatrix}^T. \tag{3B}
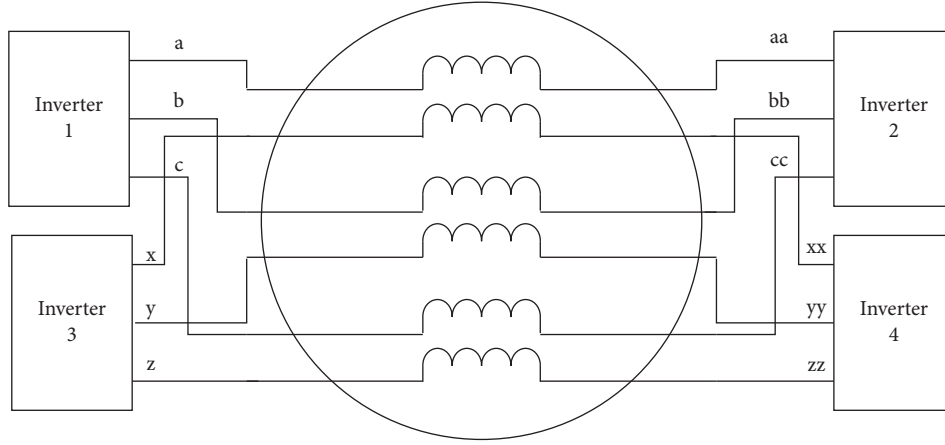$$

FIGURE 1: Open-ended winding asymmetrical six-phase induction motor connected to inverter circuits.

L is the inductance matrix as defined in the Appendix.

The electromagnetic torque, τ_e, developed is constituted from both the winding set A and X (i.e., τ_{e1}, and τ_{e1}, respectively) and is defined as

$$\tau_e = \tau_{e1} + \tau_{e2},$$
$$\tau_{e1} = c\left(i_{q1}\lambda_{d1} - i_{d1}\lambda_{q1}\right), \quad (4)$$
$$\tau_{e2} = c\left(i_{q2}\lambda_{d2} - i_{d2}\lambda_{q2}\right),$$

where $c = 3/2P/21/\omega_b$.

Rotor dynamic is given by equation (5) of the motor having P number of poles when load torque τ_l is applied. Also, p signifies the differentiation function with respect to time

$$\frac{\omega_r}{\omega_b} = \frac{1}{p}\left[\frac{1}{\omega_b}\frac{P}{2}\frac{1}{J}\left(\tau_e - \tau_l\right)\right]. \quad (5)$$

3. Indirect Field Oriented Control

Dynamic expressions of asymmetrical six-phase induction machine defined in synchronous reference frame ($\omega_k = \omega_e$) are used to develop the vector controller. Rotor equations are defined as

$$0 = r_{qr}i_{qr} + \omega_{sl}\lambda_{dr} + p\lambda_{qr}, \quad (6)$$

$$0 = r_{dr}i_{dr} - \omega_{sl}\lambda_{qr} + p\lambda_{dr}, \quad (7)$$

where

$$\omega_{sl} = \omega_e - \omega_r, \quad (8A)$$

$$\lambda_{qr} = L_{lr}i_{qr} + L_m\left(i_{q1} + i_{q2} + i_{qr}\right), \quad (8B)$$

$$\lambda_{dr} = L_{lr}i_{dr} + L_m\left(i_{d1} + i_{d2} + i_{dr}\right), \quad (8C)$$

and with the assumption of rotor flux along d axis, we have

$$\lambda_r = \lambda_{dr}, \quad (9)$$

$$\lambda_{qr} = 0, \quad (10)$$

$$p\lambda_r = 0. \quad (11)$$

Substituting equations (9)–(11) into (6) and (7) yields

$$r_{qr}i_{qr} + \omega_{sl}\lambda_r = 0, \quad (12)$$

$$r_{dr}i_{dr} + p\lambda_{dr} = 0. \quad (13)$$

Obtained value of i_{qr} and i_{dr} from equations (8B) and (8C) is substituted in equations (12) and (13) and yields

$$\omega_{sl} = K_{sl}i_T, \quad (14)$$

$$i_F = \left(1 + T_r p\right)\lambda_r, \quad (15)$$

where

$$K_{sl} = \frac{L_m}{T_r\lambda_r}, \quad (16A)$$

$$i_T = i_{q1} + i_{q2}, \quad (16B)$$

$$i_F = i_{d1} + i_{d2}, \quad (16C)$$

$$T_r = \frac{L_r}{r_r} \text{ is rotor time constant.} \quad (16D)$$

After the substitution and simplification of rotor current value into torque, the expression will result in the following:

$$\tau_e = K_T\lambda_r i_T = K_1 i_T, \quad (17)$$

$$K_1 = K_T\lambda_r \quad (18A)$$

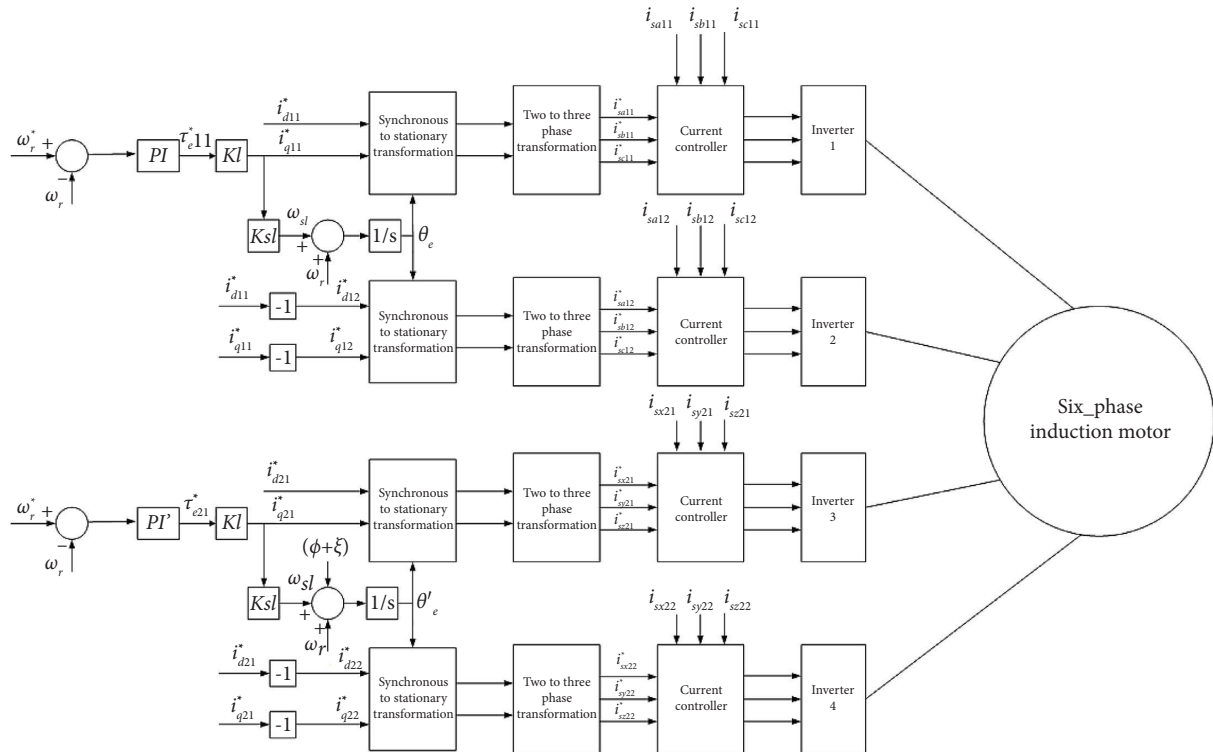$$K_T = c\frac{L_m}{L_r}. \quad (18B)$$

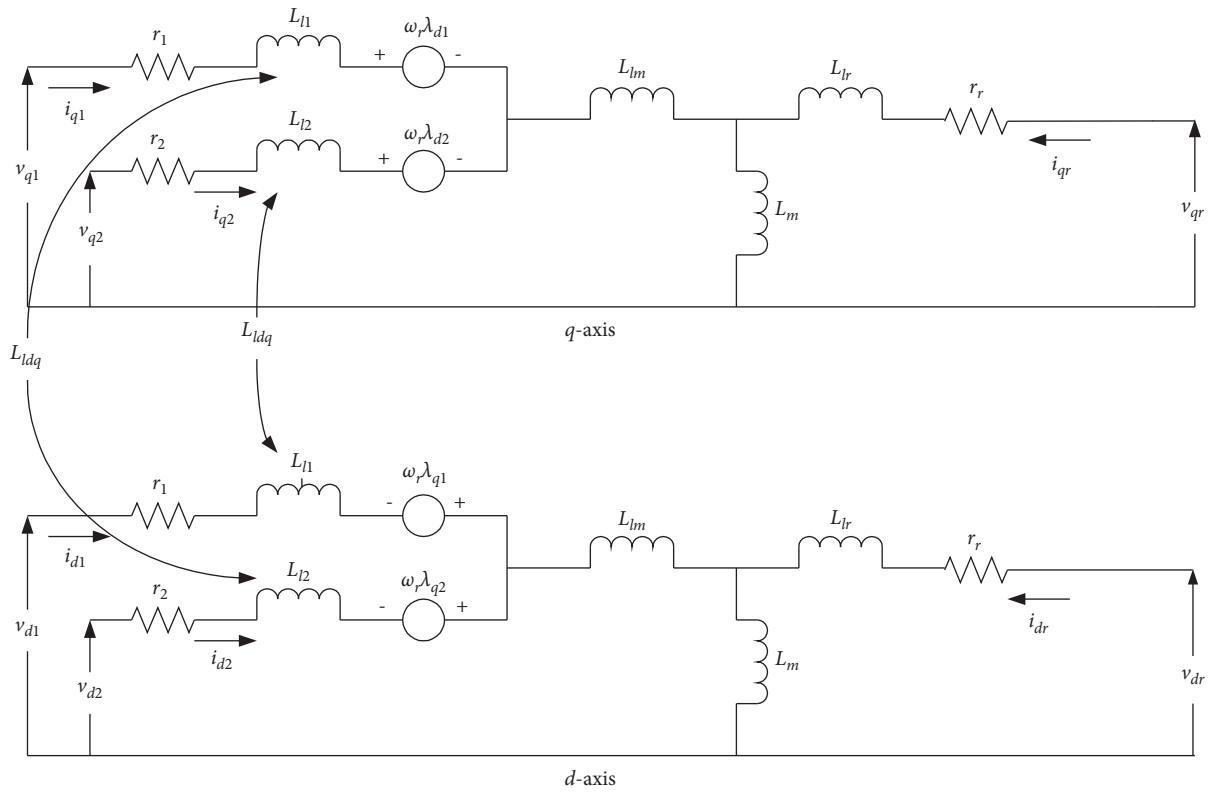FIGURE 2: Block diagram of field oriented open-ended asymmetrical six-phase induction machine.

FIGURE 3: Equivalent circuit representation of an asymmetrical six-phase induction motor.
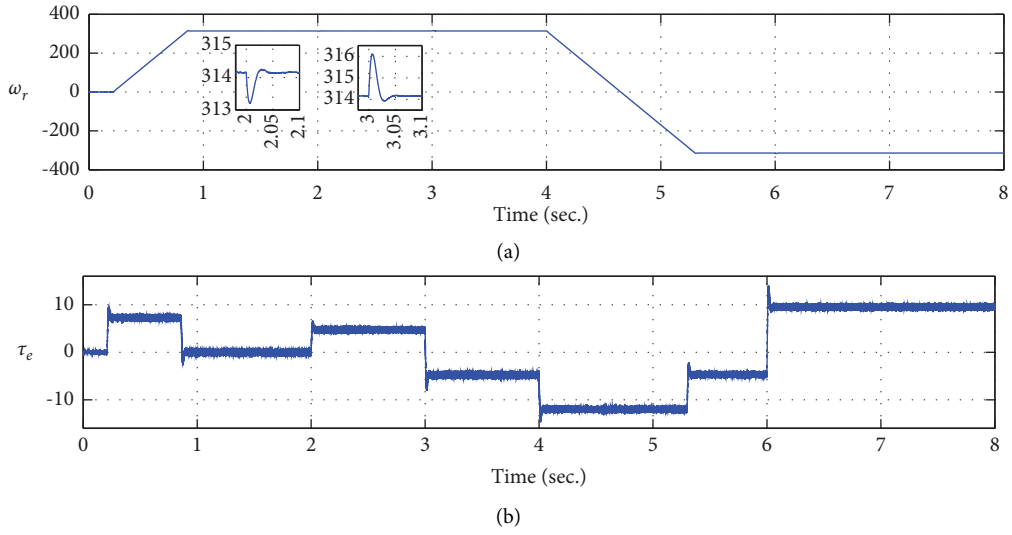
FIGURE 4: Motor response showing (a) rotor speed ω_r and (b) torque T_e.
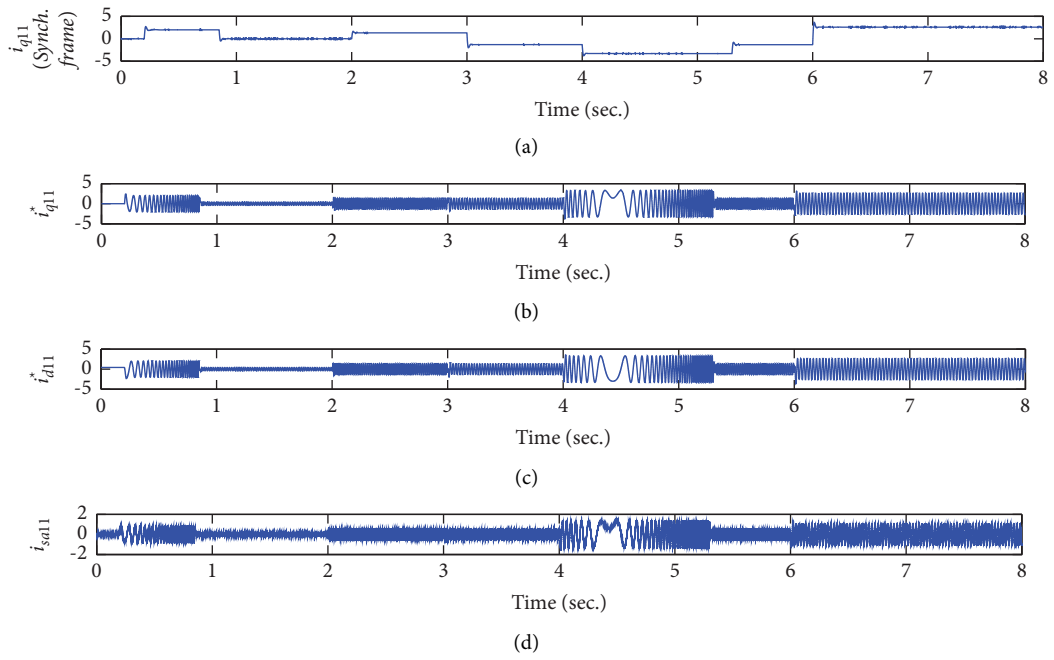

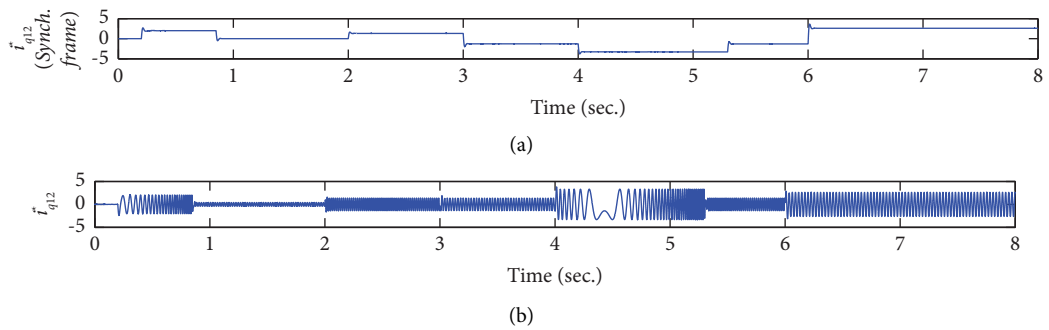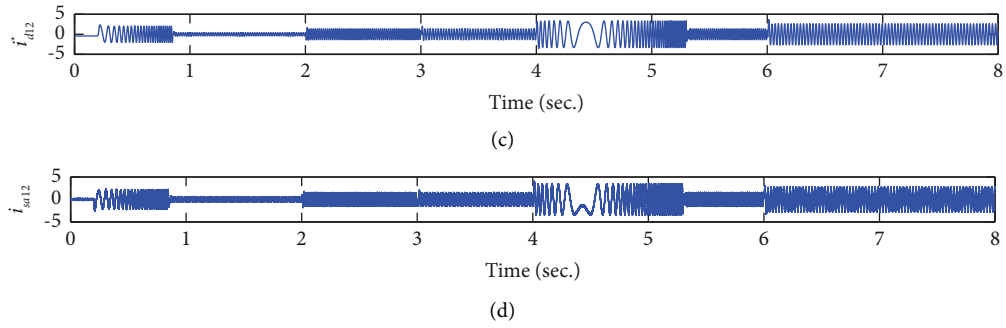FIGURE 5: Motor current through inverter 1 showing reference current.

FIGURE 6: Continued.

(c)

(d)

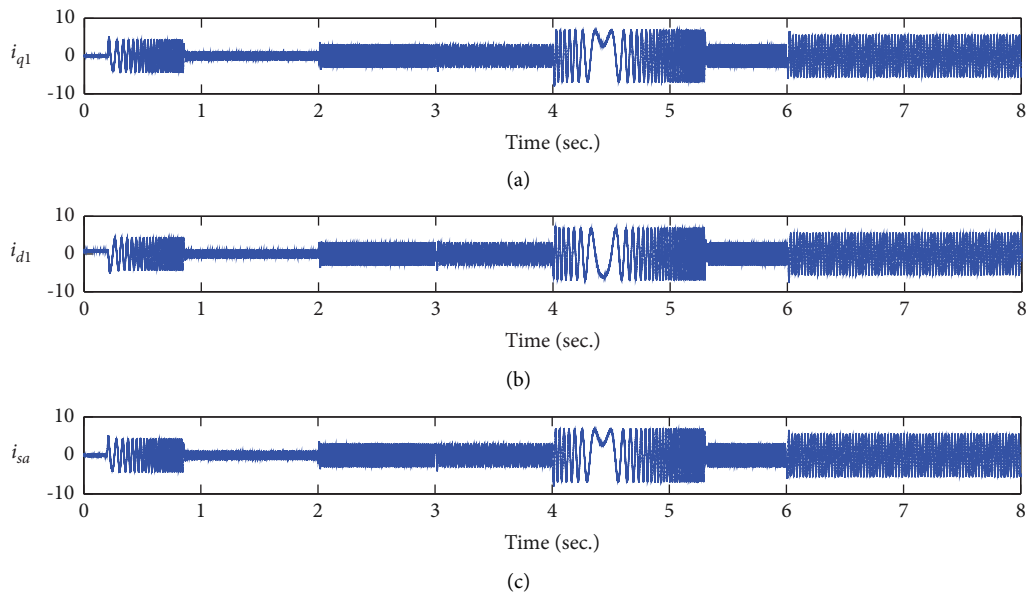FIGURE 6: Motor current through inverter 2 showing reference current.

(a)

(b)

(c)

FIGURE 7: Resultant current flowing in winding set A.

(a)

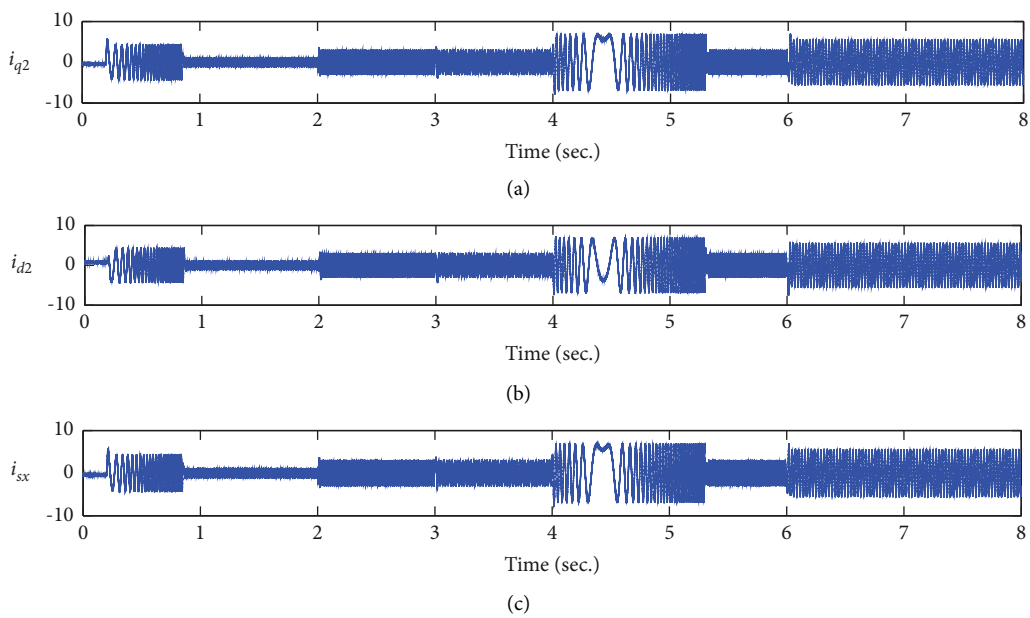(b)

(c)

FIGURE 8: Resultant current flowing in winding set X.

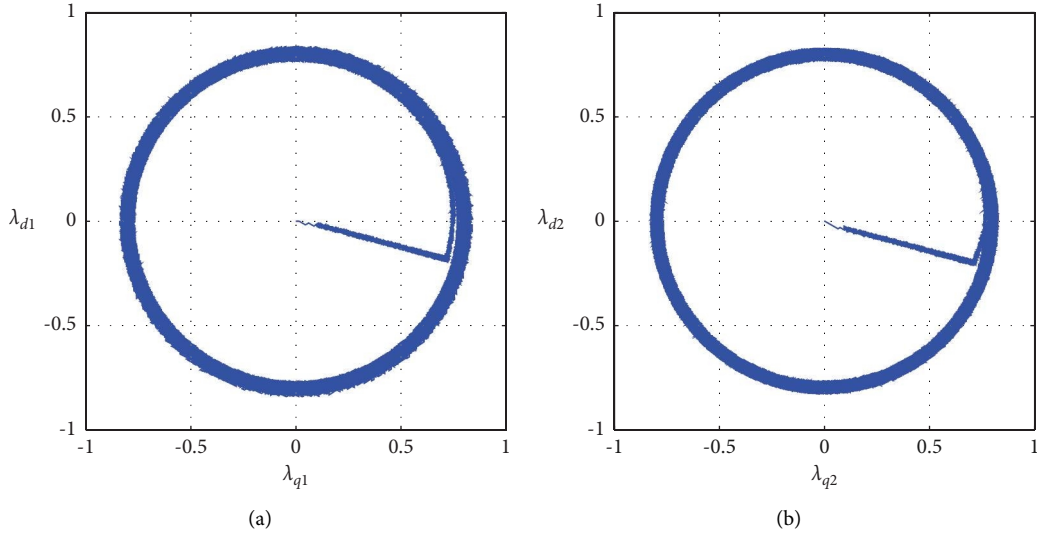(a)   (b)

FIGURE 9: Two axes flux representation of (a) winding set *A* and (b) winding set *X*.
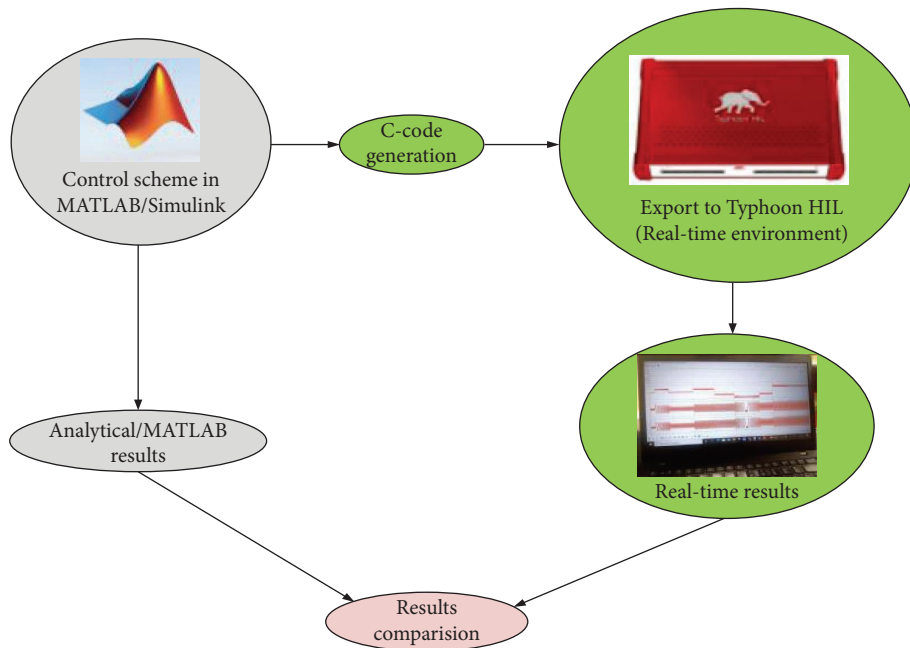

FIGURE 10: Implementation steps and set-up for real-time testing.

4. Implementation of Developed Control Scheme

The mathematically derived indirect field-oriented control scheme of asymmetrical six-phase open-ended winding induction motor is shown by the block diagram in the Figures 2 and 3. For simplicity, the motor operation has been only presented up to the base speed in constant torque region, but it may be extended to operate above base speed in field weakening region.

In the block diagram, implementation of developed control scheme is shown for each winding set *A* and *X* whose open ends are connected to inverters. Speed control loop is used to generate the reference q-component of stator current i^*_{q11} and i^*_{q21} by using a speed controller (PI controller marked as PI and PI′) which are associated with inverters 1 and 3, respectively. In the figure, i^*_{q21} (and i^*_{d21}) is obtained from a negative gain given to the generated reference current i^*_{q11} (and i^*_{d11}). This is because a phase shift of 180 degree electrical is maintained between the input supply from inverters 1 and 2 (also inverters 3 and 4). The generated torque component of current is used to obtain the rotor slip ω_{sl} using the equation (14), which is then added to rotor speed ω_r to obtain the speed of rotating reference frame, i.e., synchronous speed ω_e.
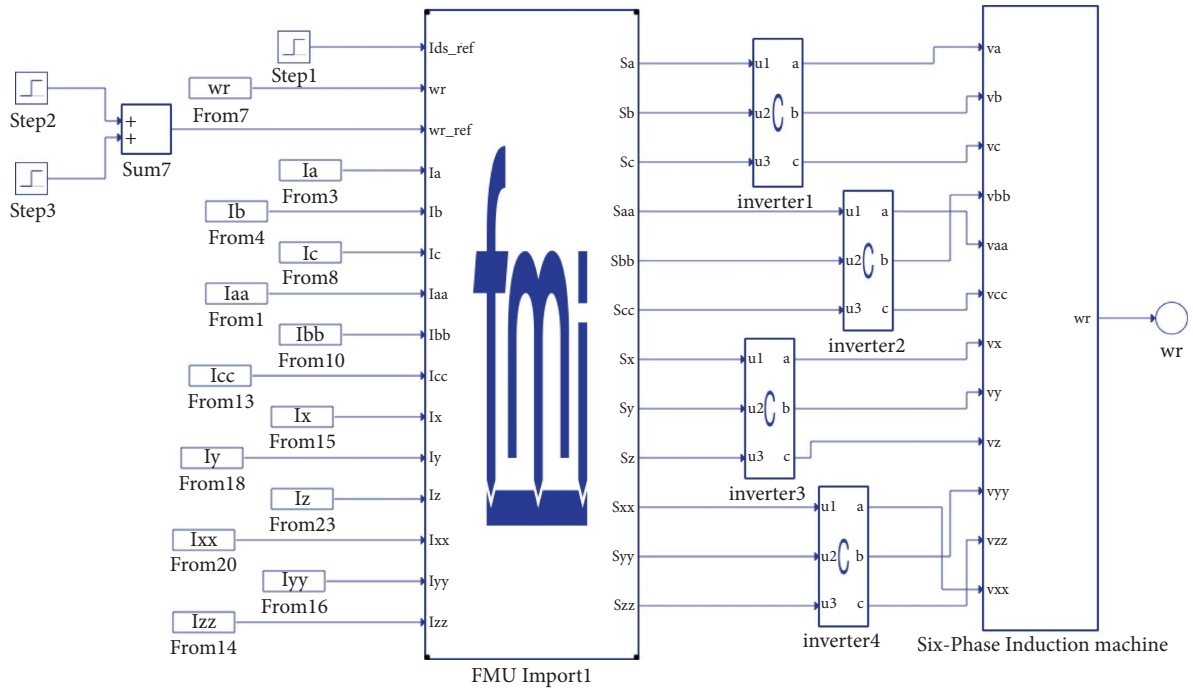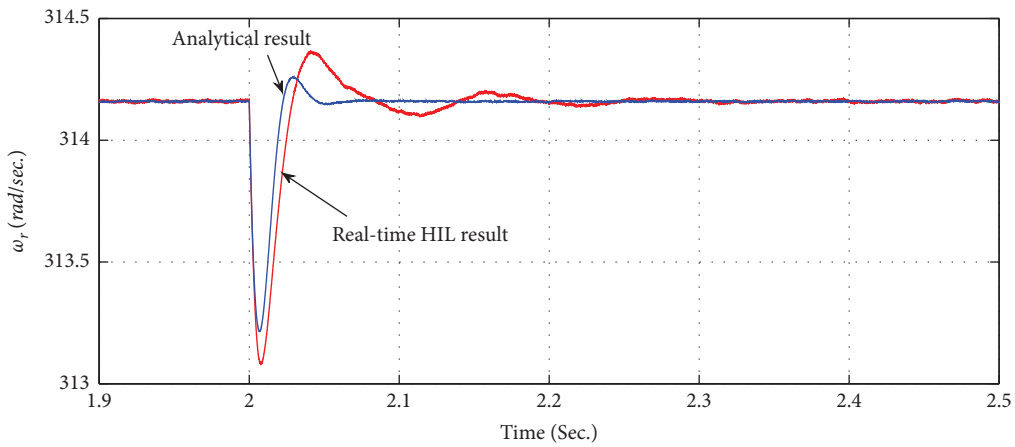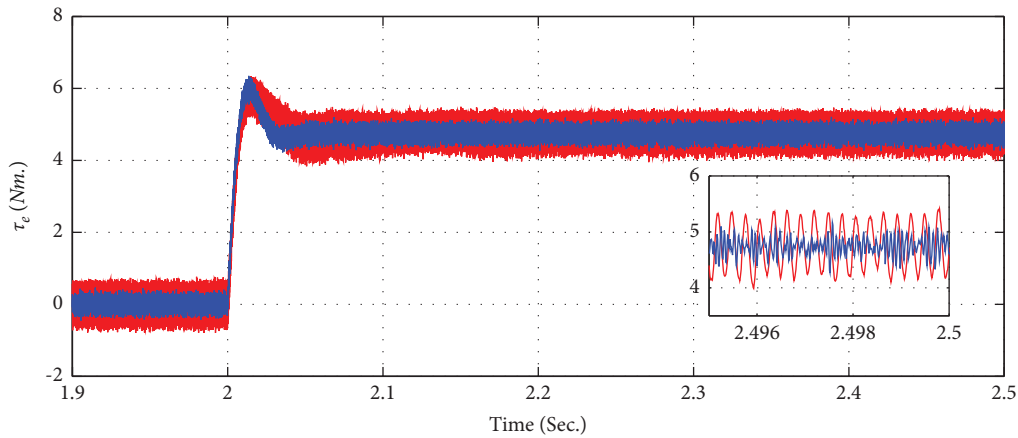
FIGURE 11: HIL testing model of the drive system.

(a)

(b)

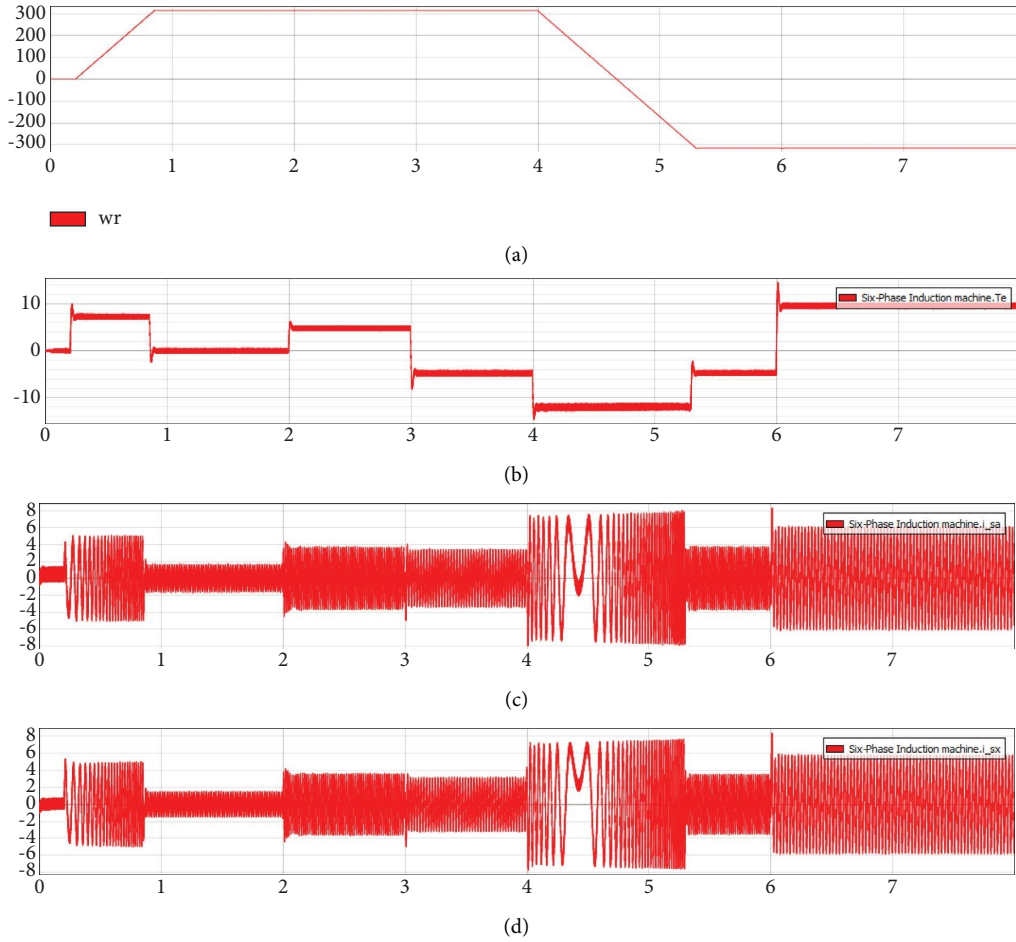FIGURE 12: Comparative results of motor showing (a) rotor speed and (b) developed torque.

FIGURE 13: Real-time test results of four quadrant operation: (a) rotor speed; (b) developed torque; (c) winding current of phase *a*; (d) winding current of phase *x*.

The above obtained reference current is transformed to stationary frame and again transformed from stationary two axes to its equivalent three-phase current [1, 24]. The angle θ_e (obtained by integrating the speed ω_e) is used for transformation purpose. Hence, the generated reference current in the stationary three-phase system is compared with the actual winding current. After comparison, the current error is inputted to the used hysteresis controller, which regulates the switching signal of inverter connected to each open-ended stator winding.

5. Analytical Results

During the analysis, it was assumed that six-phase stator winding was realized by reconfiguring the existing three-phase induction motor using the procedure explained in [25]. Initially, a ramp function speed command was initialized at time $t = 0.2$ s, and the motor starts to operate at rated speed at time $t = 0.65$ s at no-load condition. At time $t = 2.0$ s, the motor was loaded with 50% of rated/base torque, resulting in a small dip in rotor speed (by 0.9 rpm) and again regains its original commanded speed within 0.05 s, signifying the property of disturbance rejection of the developed system. Both speed and torque characteristics are

shown in Figures 4(a) and 4(b), respectively. During this condition, the machine is operating in first quadrant of torque-speed characteristic [1]. The motor current fed by the end connected inverter of winding set A and X is shown in Figures 5 and 6, respectively. In synchronous reference frame, *q*-component of current increased to 1.315 A. The *d-q* component of current in stationary reference frame together with complete waveform of current i_{sa11} and i_{sa12} is also shown in the figure. During the motor operation, field weakening region was not considered and excitation current (i.e., *d*-component of stator current) was maintained constant. It may be noted here that the active component of stator current contributed by inverters 1 and 2 is equal, indicating an equal power sharing by both the connected inverters. A similar explanation may also be given for currents in winding set X. For the operation of motor in second quadrant, the torque direction was reversed at time $t = 3$ s. This resulted in an increase in rotor speed by small amount (by 1.9 rpm) but again regains its commanded speed within 0.05 s, as shown in zoomed view of Figure 4(a). The active component of current by each connected inverters in winding set A and X was found to be 1.294 A (in magnitude). At time $t = 4$ s, ramp function rotor speed command was initialized for the operation in third quadrant (reverse
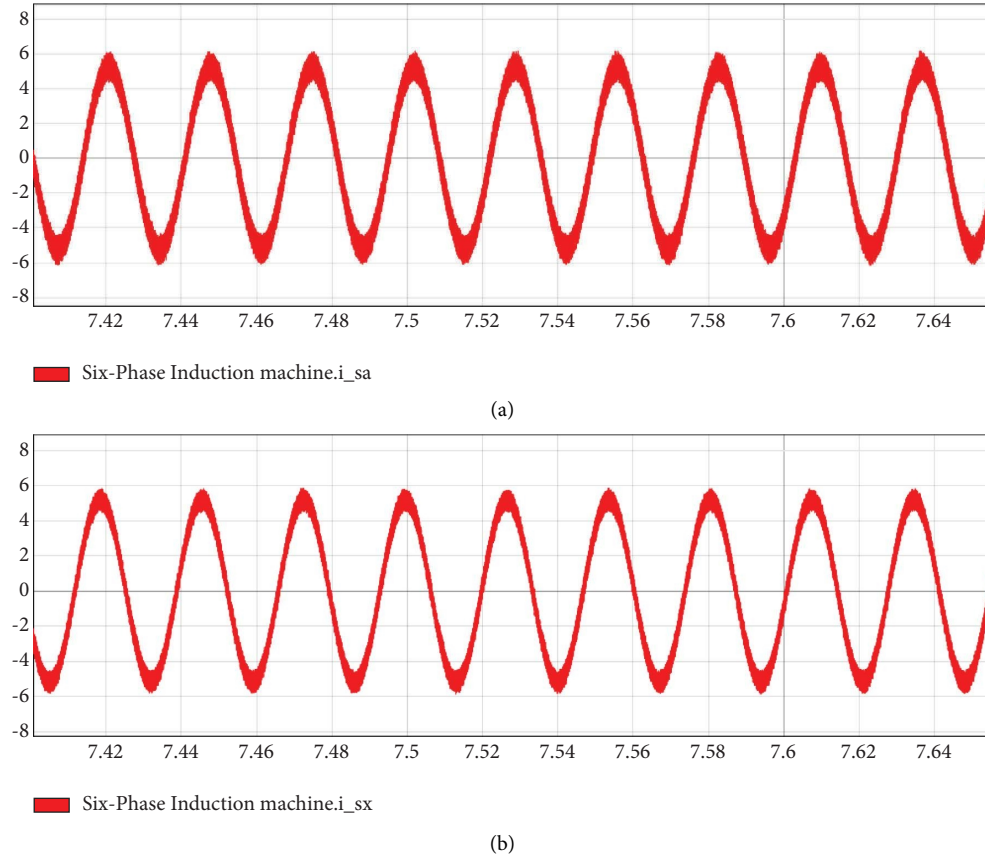
Six-Phase Induction machine.i_sa

(a)

Six-Phase Induction machine.i_sx

(b)

FIGURE 14: Real-time test results during steady-state operation: (a) winding current of phase *a*; (b) winding current of phase *x*.

FIGURE 15: Experimental set-up used during real-time testing.

motoring mode). During this mode, the q-component of current (i.e., i_{q11} and i_{q12}) was found to be 1.317 A (in magnitude). Furthermore, at time $t = 6$ s, the direction of torque was again reversed to shift the operational mode to fourth quadrant. During this condition, steady-state active component of inverter current was found to be 2.60 A. Since the flow of stator current in particular winding set A or X is constituted by two end connected inverters, this resultant current together with the d-q component in stationary reference frame is shown in Figures 7 and 8. Flux in the machine due to the flow of resultant current has also been

depicted in Figures 9(a) and 9(b), associated with winding set A and X, respectively.

6. Validation Using HIL Testing

Implementation of the complete developed system was tested in real-time environment by using a Typhoon HIL 402 emulator. In the machine drive system, closed loop control scheme (i.e., indirect field-oriented control) initially developed in MATLAB/Simulink was tested in real-time platform by importing their generated C-code
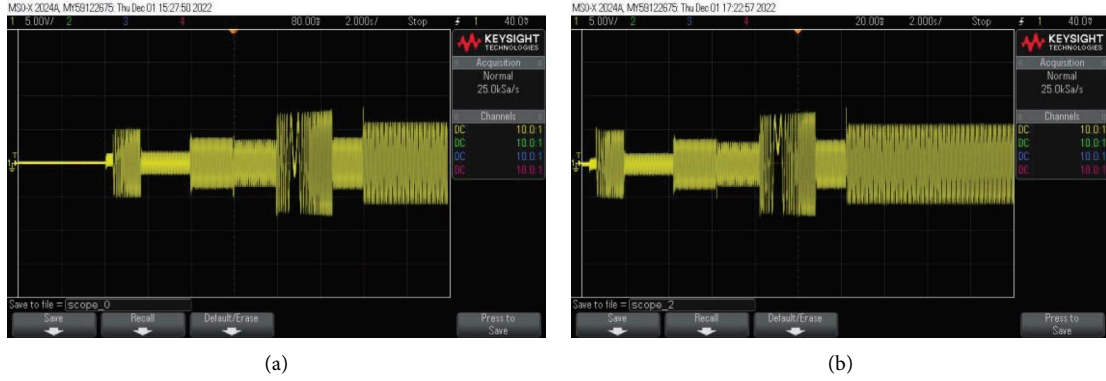
(a)

(b)

Figure 16: Experimental test results of four quadrant operation: (a) winding current of phase *a*; (b) winding current of phase *x*.
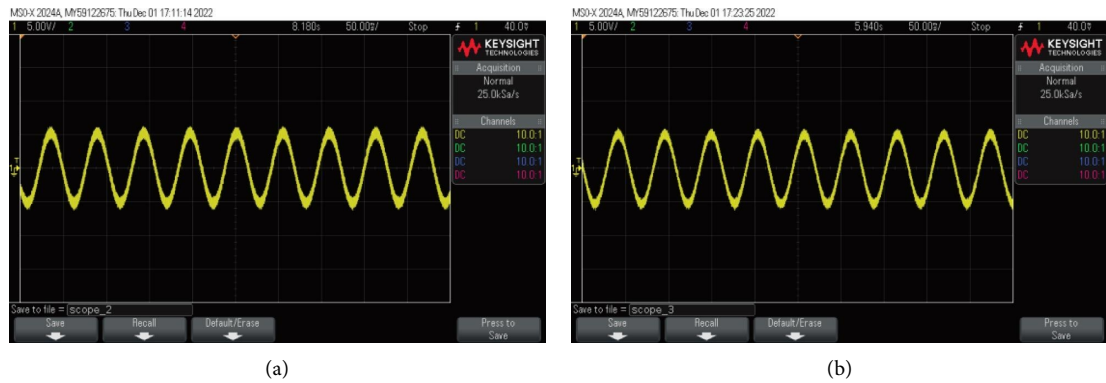

(a)

(b)

Figure 17: Experimental test results during steady-state operation: (a) winding current of phase *a*; (b) winding current of phase *x*.

to HIL emulator through functional mock-up interface (FMI) block [26]. During the import process, C-code together with binaries and XML files are zipped to a single file, known as FMU (functional mock-up unit). All procedural implementation steps for both analytical and real-time test results are shown in Figure 10. The model developed by using schematic editor to obtain real-time results is shown in Figure 11; wherein, FMI block is used to interface the simulation model with real-time environment of Typhoon HIL.

The presented analytical results in previous section have been validated for the machine operation in the motoring mode only (i.e., in the first quadrant operation). The rotor behavior of the developed model is shown in Figure 12. Both responses of speed are matching, and an inevitable larger dip in rotor speed was noted by 0.96 and 0.76 rad/s, approximately in analytical and real-time HIL results, as shown in Figure 12(a). A comparative torque response is shown in Figure 12(b). In both speed-torque responses, some higher pulsation in real-time HIL result was noted particularly to be torque under steady-state and is visualized in zoomed portion of figure. It may be accounted for the consideration of various nonideal factors and simplifying assumption in real-time test results. Complete four quadrant responses of both stator and rotor side are shown in Figure 13. Operation during steady-state (in fourth quadrant after time $t = 6$ s) is

also shown, where current in one of the phase winding of set A and X (i.e. i_{sa} and i_{sx}) is depicted in Figures 14(a) and 14(b), respectively. The experimental set-up used to obtain hardware results is shown in Figure 15. In this set-up, a digital signal oscilloscope (DSO) is used to capture the response of the system. Captured dynamic responses of current i_{sa} and i_{sx} are shown in Figures 16(a) and 16(b), respectively. These current responses are matching with both analytical (i.e., Figures 7(c) and 8(c), respectively) and real-time simulation results (i.e., Figures 13(c) and 13(d), respectively). Captured steady-state responses of current i_{sa} and i_{sx} are also shown in Figures 17(a) and 17(b), respectively. A closed agreement of captured steady-state current may be noted with real-time simulation results of Figures 14(a) and 14(b), respectively.

7. Conclusions

In this study, a simple indirect field-oriented control, i.e., vector control has been developed for asymmetrical six-phase open-ended winding induction motor. The proposed model with its control has been developed under MATLAB/ Simulink environment. The developed scheme facilitates an independent control of torque and flux component of current, hence substantially improving the dynamic characteristic of developed motor drive in four quadrant

operation. Practical suitability of the developed analytical model has been validated and tested through real-time HIL results. Both analytical results are matching with a slight mismatch because of the inclusion of various nonideal factors and simplifying assumption in real-time environment.

Presented analytical treatment with their real-time results may be further extended to various applications with other multiple three-phase machines, particularly nine phases. Further work may also deal with both synchronous and asynchronous machine. A comparative performance investigation with different rating machine will be taken up for further investigation as an extension of the present work.

Appendix

Parameters of 2 HP 4 poles induction motor are given:

$$r_1 = 5.0 \ \Omega \qquad r_2 = 5.0 \ \Omega \qquad r_r = 3.15 \ \Omega$$

$$L_{lr} = 0.02 \, \text{H} \qquad L_m = 0.21 \ \text{H} \qquad L_{ldq} = 0 \ \text{H}$$

$$L_{l1} = L_{l2} = 0.02 \ \Omega \qquad L_{lm} = 0.002 \, \text{H}$$

$$J = 0.03 \ Kgm^2$$

$$L = \begin{bmatrix} (x_{l1} + x_{lm} + x_{md}) & 0 & (x_{lm} + x_{md}) & x_{ldq} & x_{md} & 0 & x_{md} \\ 0 & (x_{l1} + x_{lm} + x_{md}) & -x_{ldq} & (x_{lm} + x_{mq}) & 0 & x_{mq} & 0 \\ (x_{lm} + x_{md}) & -x_{ldq} & (x_{l2} + x_{lm} + x_{md}) & 0 & x_{md} & 0 & x_{md} \\ x_{ldq} & (x_{lm} + x_{mq}) & 0 & (x_{l2} + x_{lm} + x_{mq}) & 0 & x_{mq} & 0 \\ x_{md} & 0 & x_{md} & 0 & (x_{lKd} + x_{md}) & 0 & x_{md} \\ 0 & x_{mq} & 0 & x_{mq} & 0 & (x_{lKq} + x_{mq}) & 0 \\ x_{md} & 0 & x_{md} & 0 & x_{md} & 0 & (x_{lfr} + x_{md}) \end{bmatrix}$$

$$v_{sa} = v_{sa11} - v_{sa12} \qquad i_{sa} = i_{sa11} - i_{sa12}$$

$$v_{sb} = v_{sb11} - v_{sb12} \qquad i_{sb} = i_{sb11} - i_{sb12}$$

$$v_{sc} = v_{sc11} - v_{sc12} \qquad i_{sc} = i_{sc11} - i_{sc12}$$

$$v_{sx} = v_{sx21} - v_{sx22} \qquad i_{sx} = i_{sx21} - i_{sx22}$$

$$v_{sy} = v_{sy21} - v_{sy22} \qquad i_{sy} = i_{sy21} - i_{sy22}$$

$$v_{sz} = v_{sz21} - v_{sz22} \qquad i_{sz} = i_{sz21} - i_{sz22}$$

$$v_{d1} = v_{d11} - v_{d12} \qquad i_{d1} = i_{d11} - i_{d12}$$

$$v_{q1} = v_{q11} - v_{q12} \qquad i_{q1} = i_{q11} - i_{q12}$$

$$v_{d2} = v_{d21} - v_{d22} \qquad i_{d2} = i_{d21} - i_{d22}$$

$$v_{q2} = v_{q21} - v_{q22} \qquad i_{q2} = i_{q21} - i_{q22}$$

v_{sa11}, v_{sb11}, v_{sc11} are the simple voltage inverter 1, v_{sa12}, v_{sb12}, v_{sc12} are the simple voltage inverter 2, v_{sx21}, v_{sy21}, v_{sz21} are the simple voltage inverter 3, v_{sx22}, v_{sy22}, v_{sz22} are the simple voltage inverter 4, and v_{d11}, v_{q11}, and v_{d12}, v_{q12} are the d-q voltage components of inverter 1 and inverter 2, respectively. Similarly, v_{d21}, v_{q21}, and v_{d22}, v_{q22} are the d-q voltage components of inverter 3 and inverter 4, respectively.

Data Availability

The data used to support the findings of this study are available from the corresponding author upon request.

Conflicts of Interest

The authors declare that they have no conflicts of interest.

References

[1] B. K. Bose, *Modern Power Electronics and AC Drives*, Prentice Hall PTR, Upper Saddle River, NJ, USA, 2002.

[2] G. K. Singh, "Multiphase induction machine drive research-A survey," *Electric Power Systems Research*, vol. 61, no. 2, pp. 139–147, 2002.

[3] S. Ansari, J. Zhang, and R. E. Singh, "A review of stabilization methods for DCMG with CPL, the role of bandwidth limits and droop control," *Prot Control Mod Power Syst*, vol. 7, pp. 2–12, 2023.

[4] Y. F. Jia, N. Xu, L. Chu et al., "Control strategy for an open-end winding induction motor drive system for dual-power electric vehicles," *IEEE Access*, vol. 8, pp. 8844–8860, 2020.

[5] P. Srinivasan, B. L. Narasimharaju, and N. V. Srikanth, "Space-vector pulse width modulation scheme for open-end winding induction motor drive configuration," *IET Power Electronics*, vol. 8, no. 7, pp. 1083–1094, 2015.

[6] P. H. Kumar, D. Mishra, S. Lakhimsetty, and V. T. Somasekhar, "A space vector PWM scheme for an open-end winding induction motor drive with a reduced power loss," *International Transactions on Electrical Energy Systems*, vol. 31, no. 11, Article ID e13104, 2021.

[7] S. Lakhimsetty, P. Hema Kumar, and V. T. Somasekhar, "Hybrid space-vector pulse width modulation strategies for a four-level open-end winding induction motor drive with an improvised harmonic performance and balanced DC-link capacitors," *International Transactions on Electrical Energy Systems*, vol. 31, no. 4, Article ID e12814, 2021.

[8] I. J. Smith and J. Salmon, "High-efficiency operation of an open-ended winding induction motor using constant power factor control," *IEEE Transactions on Power Electronics*, vol. 33, no. 12, pp. 10663–10672, 2018.

[9] N. R. Kedika and S. Pradabane, "Fault-tolerant multi-level inverter topologies for open-end winding induction motor drive," *International Transactions on Electrical Energy Systems*, vol. 31, no. 2, Article ID e12718, 2021.

[10] I. J. Smith and J. Salmon, "High-efficiency operation of an open-ended winding induction motor using constant power factor control," *IEEE Transactions on Power Electronics*, vol. 33, no. 12, pp. 10663–10672, 2018.

[11] A. Amerise, M. Mengoni, L. Zarri, A. Tani, S. Rubino, and R. Bojoi, "Open-end windings induction motor drive with floating capacitor bridge at variable DC-link voltage," *IEEE Transactions on Industry Applications*, vol. 55, no. 3, pp. 2741–2749, 2019.

[12] K. V. Praveen Kumar, K. M. Ravi Eswar, and T. V. Kumar, "Hardware implementation of predictive torque controlled open-end winding induction motor drive with self-tuning algorithm," *Cogent Engineering*, vol. 4, no. 1, Article ID 1388206, 2017.

[13] R. E. Kodumur Meesala, V. P. K. kunisetti, and V. Kumar Thippiripati, "Enhanced predictive torque control for open end winding induction motor drive without weighting factor assignment," *IEEE Transactions on Power Electronics*, vol. 34, no. 1, pp. 503–513, 2019.

[14] E. Levi, I. N. W. Satiawan, N. Bodo, and M. Jones, "A space-vector modulation scheme for multilevel open-end winding five-phase drives," *IEEE Transactions on Energy Conversion*, vol. 27, no. 1, pp. 1–10, 2012.

[15] S. Guizani, A. Nayli, and F. Ben Ammar, "Comparison between star winding and open-end winding induction machines," *Electrical Engineering*, vol. 98, no. 3, pp. 219–232, 2016.

[16] N. Bodo, E. Levi, and M. Jones, "Investigation of carrier-based PWM techniques for a five-phase open-end winding drive topology," *IEEE Transactions on Industrial Electronics*, vol. 60, no. 5, pp. 2054–2065, 2013.

[17] S. Guizani and F. Ben Ammar, "Dual open-end stator winding induction machine fed by redundant voltage source inverters," *Turkish Journal of Electrical Engineering and Computer Sciences*, vol. 23, pp. 2171–2181, 2015.

[18] G. K. Singh, K. Nam, and S. K. Lim, "A simple indirect field oriented control scheme for multiphase induction machine," *IEEE Transactions on Industrial Electronics*, vol. 52, no. 4, pp. 1177–1184, 2005.

[19] E. Levi, "Multiphase electric machines for variable-speed applications," *IEEE Transactions on Industrial Electronics*, vol. 55, no. 5, pp. 1893–1909, 2008.

[20] W. Grega, "Hardware-in-the-loop simulation and its application in control education," in *Proceedings of the FIE'99 Frontiers in Education. 29th Annual Frontiers in Education Conference. Conference Proceedings (IEEE Cat. No.99CH37011)*, pp. 12B6/7–12B612, San Juan, PR, USA, November, 1999.

[21] A. Iqbal, G. K. Singh, and V. Pant, "Steady-state modeling and analysis of six-phase synchronous motor," *Systems Science & Control Engineering*, vol. 2, no. 1, pp. 236–249, 2014.

[22] A. Iqbal and G. K. Singh, "Modeling and stability analysis of three- and six-phase asymmetrical grid-connected induction generator," *Electrical Engineering*, vol. 103, no. 2, pp. 1169–1181, 2021.

[23] A. Iqbal and G. K. Singh, "PSO based controlled six-phase grid connected induction generator for wind energy generation," *CES Transactions on Electrical Machines and Systems*, vol. 5, no. 1, pp. 41–49, 2021.

[24] P. C. Krause, O. Wasynczuk, and S. D. Sudhoff, *Analysis of Electrical Machinery and Drive Systems*, John Wiley & Sons, Hoboken, NJ, USA, 2004.

[25] R. Bojoi, M. Lazzari, F. Profumo, and A. Tenconi, "Digital field-oriented control for dual three-phase induction motor drives," *IEEE Transactions on Industry Applications*, vol. 39, no. 3, pp. 752–760, 2003.

[26] Typhoon-hil, "Typhoon-hil documentation," https://www.typhoon-hil.com/documentation/typhoon-hil-software-manual/References/fmu_import.html?hl=fmu.